MITSUBISHI ELECTRIC RESEARCH LABORATORIES
https://www.merl.com

Torque Constraint Modeling and Reference Shaping for Servo Systems

Lu, Zehui; Zhang, Tianpeng; Wang, Yebin

TR2025-006 January 08, 2025

Abstract

Servo systems, one of the backbones of modern manufacturing, are supposed to move as fast as possible for high productivity. Due to the inaccurate information on torque capacity, conventional trajectory generation methods are either overly conservative, compromising yield, or violate dynamical feasibility, compromising quality. This work proposes a method to address these shortcomings. Stable adaptive estimation of the servomotor model parameters is first performed, then torque capacity constraints are established as analytical functions of the motor speed based on parameter estimates, and finally, a computationally efficient algorithm is developed to reshape an aggressive (dynamically infeasible) trajectory into a feasible one. Theoretical analysis and numerical simulation validate the effectiveness of the proposed method.

IEEE Control Systems Letters (L-CSS) 2024

Mitsubishi Electric Research Laboratories, Inc.
201 Broadway, Cambridge, Massachusetts 02139

Torque Constraint Modeling and Reference Shaping for Servo Systems

Zehui Lu, Tianpeng Zhang, and Yebin Wang

***Abstract*— Servo systems, one of the backbones of modern manufacturing, are supposed to move as fast as possible for high productivity. Due to the inaccurate information on torque capacity, conventional trajectory generation methods are either overly conservative, compromising yield, or violate dynamical feasibility, compromising quality. This work proposes a method to address these shortcomings. Stable adaptive estimation of the servomotor model parameters is first performed, then torque capacity constraints are established as analytical functions of the motor speed based on parameter estimates, and finally, a computationally efficient algorithm is developed to reshape an aggressive (dynamically infeasible) trajectory into a feasible one. Theoretical analysis and numerical simulation validate the effectiveness of the proposed method.**

I. Introduction

Servomotor systems that perform point-to-point positioning tasks are widely used in many manufacturing applications, such as robotic manipulators and lithography machines. Controlling a servo system typically includes two stages, i.e., trajectory generation [1]–[7], and motor control (tracking) [7]–[11]. In the first stage, usually an optimization problem is formulated to find an optimal reference motion trajectory while minimizing an objective function (e.g., time or energy optimal) and satisfying the motor's dynamical constraints [2], [3]. In the second stage, the reference trajectory is fed into a motor tracking controller as the desired trajectory, and the motor tracking controller adjusts the motor current and voltage to achieve the desired torque.

Although one could formulate a complex optimization problem with dynamics constraints to generate a dynamically feasible trajectory, deploying such algorithms on machines with limited computational resources is challenging. Some servomotor control methods aim to reduce the computational burden for trajectory generation by trajectory parameterization given maximum acceleration and velocity [1], simplifying the dynamics as linear system [3], [4], and reference/command governor [5], [6], [12]. Some methods use simplistic trajectories incorporating limited dynamical information or physical constraints from the motor (actuator). Although such methods are computationally efficient, the resulting reference trajectories may not be dynamically feasible or may violate motor physical constraints. The tracking controller cannot achieve the desired states specified by such reference trajectories, yielding significant tracking errors. To prevent constraint violation of these trajectories, a common method is to limit the maximum acceleration and velocity of the generated trajectories to prevent overly aggressive and potentially infeasible motion. However, this remedy results in conservative motion and reduces productivity.

This paper proposes a computationally efficient close-loop motion planning and control framework for servo systems. The framework is designed to balance two conflicting requirements: dynamical feasibility and computational efficiency. It also addresses the challenge of imperfect prior knowledge of motor parameters. The proposed framework includes three key components: a motor parameter adaptive estimator, a motor torque capacity modeling module, and a reference reshaper (RR). Given a potentially infeasible reference trajectory generated by an arbitrary motion planner, the RR adjusts it to satisfy dynamic and physical constraints. The adaptive estimator and torque capacity modeling module update the motor's physical parameters based on the observed input/output values and feed this physical information to the RR in real time. All three components are designed to be efficient enough to be computed in real time during the motor's operation.

II. Problem Formulation

This paper considers the servomotor system of a work tool driven by a Surface-Mounted Permanent Magnet Synchronous Motor (SPMSM), where the work tool moves on a one-dimensional line. Table I summarizes the system states and parameters. The motor's states are constrained by

$$i_{\mathrm{d}}^2 + i_{\mathrm{q}}^2 \le I_{\max}^2,\ u_{\mathrm{d}}^2 + u_{\mathrm{q}}^2 \le V_{\mathrm{dq,max}}^2, \tag{1a}$$

$$-\omega_{\mathrm{m}}(\boldsymbol{\beta}) \le \omega \le \omega_{\mathrm{m}}(\boldsymbol{\beta}), \tag{1b}$$

where $V_{\mathrm{dq,max}} \triangleq V_{\max}/\sqrt{3} - RI_{\max} > 0$ is the maximum voltage drop to overcome back-EMF (counter-electromotive force); $\omega_{\mathrm{m}}(\boldsymbol{\beta})$ is the motor's max angular velocity, which is a function of motor parameters $\boldsymbol{\beta}$. The following model describes the system dynamics when the states satisfy (1):

$$\dot{\boldsymbol{x}} = \begin{bmatrix} \dot{i}_{\mathrm{d}} \\ \dot{i}_{\mathrm{q}} \\ \dot{\omega} \\ \dot{s} \\ \dot{v} \end{bmatrix} = \begin{bmatrix} \frac{1}{L_{\mathrm{d}}}(-Ri_{\mathrm{d}} + p\omega L_{\mathrm{q}} i_{\mathrm{q}} + u_{\mathrm{d}}) \\ \frac{1}{L_{\mathrm{q}}}(-Ri_{\mathrm{q}} - (L_{\mathrm{d}} i_{\mathrm{d}} + \Phi_{\mathrm{pm}})p\omega + u_{\mathrm{q}}) \\ J^{-1} 1.5 p \Phi_{\mathrm{pm}} i_{\mathrm{q}} \\ v \\ 1.5 p \Phi_{\mathrm{pm}} i_{\mathrm{q}} Z \end{bmatrix}, \tag{2}$$

where $\boldsymbol{x} \triangleq \begin{bmatrix} i_{\mathrm{d}} & i_{\mathrm{q}} & \omega & s & v \end{bmatrix}^\top \in \mathbb{R}^5$ is the system state, $\boldsymbol{u} \triangleq \begin{bmatrix} u_{\mathrm{d}} & u_{\mathrm{q}} \end{bmatrix}^\top \in \mathbb{R}^2$ is the control input and $Z > 0$

Z. Lu is with the School of Aeronautics and Astronautics, Purdue University, IN 47907, USA. Email: lu846@purdue.edu

T. Zhang is with the Harvard School of Engineering and Applied Sciences, MA 02138 USA. Email: tzhang@g.harvard.edu

Y. Wang is with Mitsubishi Electric Research Laboratories (MERL), Cambridge, MA 02139, USA. Email: yebinwang@ieee.org

This work was done while Z. Lu and T. Zhang were interns at MERL.

TABLE I

SYMBOLS USED IN THE SPMSM MODEL

Symbol	Description	Sym.	Description
$L_\mathrm{d}, L_\mathrm{q}$	inductance in d- and q-axis	ω	rotor angular velocity
$i_\mathrm{d}, i_\mathrm{q}$	current in d- and q-axis	s	work tool position
$u_\mathrm{d}, u_\mathrm{q}$	voltage in d- and q-axis	v	work tool velocity
Φ_pm	permanent magnet flux	J	rotor + load inertia
V_max	max DC bus voltage	p	number of pole pairs
I_max	max current	R	winding resistance

Subscript $_\mathrm{des}$ indicates desired value; hat $\hat{}$ indicates value estimate; tilde $\tilde{}$ indicates estimate error

is a known gear ratio. Note that $v = ZJ\omega$ according to (2). We assume we know the values of $p, V_\mathrm{max}, I_\mathrm{max}, R$ accurately, but our knowledge about the parameter values in $\boldsymbol{\beta} \triangleq \begin{bmatrix} L_\mathrm{d} & L_\mathrm{q} & \Phi_\mathrm{pm} \end{bmatrix}^\top \in \mathbb{R}^3$ may be inaccurate. For the remainder of this paper, we denote $\tau \triangleq 1.5p\Phi_\mathrm{pm} i_\mathrm{q}$ as the motor torque and $a \triangleq \dot{v} = \tau Z$ as the work tool acceleration.

Remark 1. *This paper does not account for opposing torque loads, such as those caused by cutting materials, as aggressive motion is only required before or after cutting. Opposing torque loads lead to reduced motor torque and acceleration, which would not violate the constraints.*

Remark 2. *Although the winding resistance R may fluctuate with temperature, we treat it as a fixed parameter for two reasons: 1) introducing fluctuating R renders the persistent excitation more challenging to meet; 2) the fluctuation typically contributes to only ∼1% of torque capacity uncertainty.*

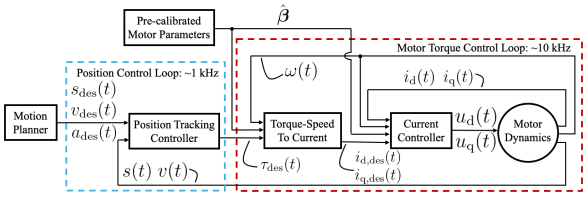

Fig. 1. The prevailing closed-loop planning and control system.

The problem of interest is to design a real-time motion planning strategy to drive the work tool to a specified location $p_\mathrm{T} \in \mathbb{R}$ as quickly as possible. Fig. 1 illustrates a common baseline method for this problem. The method first uses a simple motion planner, typically running at 1kHz, to generate a reference trajectory for the work tool to reach a target position $p_\mathrm{T} \in \mathbb{R}$ [1]–[3]. To meet the 1kHz planning frequency, the simple motion planner generally does not include dynamical information or physical constraints for computational efficiency, and the generated reference trajectories may violate the constraints in (1).Then, a motor tracking controller running at 10kHz attempts to track the reference trajectory under the physical/dynamic constraints, given a set of pre-calibrated motor parameters. The performance of such baseline methods may be lacking if the reference trajectory heavily deviates from the feasible region or if the motor parameters are inaccurate. This paper aims to propose a method that overcomes the limitations of the baseline method by reshaping the potentially infeasible reference trajectory generated by the simple motion planner to satisfy the physical/dynamic constraints and also estimates the motor parameters adaptively, which jointly results in more accurate tracking.

III. METHODOLOGY

This section presents the proposed framework, which, compared with the baseline method, additionally includes an adaptive parameter estimator, a motor torque capacity modeling module, and a reference reshaper, as illustrated in Fig. 2. Details about each component are provided below.

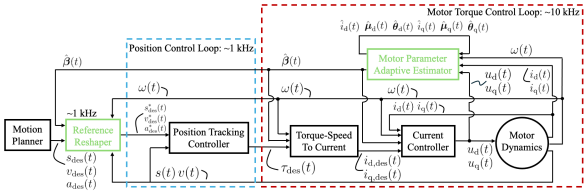

Fig. 2. The proposed closed-loop planning and control system.

A. Adaptive Parameter Estimator

The motor model parameters $\boldsymbol{\beta} = \begin{bmatrix} L_\mathrm{d} & L_\mathrm{q} & \Phi_\mathrm{pm} \end{bmatrix}^\top$ may be unknown or varying during operation, and thus the proposed reference reshaper must adapt to these changes. From (2), the system is nonlinearly parameterized. Reparameterize the motor model parameters that need to be estimated as $\boldsymbol{\theta} \triangleq \begin{bmatrix} \boldsymbol{\theta}_\mathrm{d}^\top & \boldsymbol{\theta}_\mathrm{q}^\top \end{bmatrix}^\top \in \mathbb{R}^5$, where $\boldsymbol{\theta}_\mathrm{d} \triangleq \begin{bmatrix} \frac{1}{L_\mathrm{d}} & \frac{L_\mathrm{q}}{L_\mathrm{d}} \end{bmatrix}^\top \in \mathbb{R}^2$ and $\boldsymbol{\theta}_\mathrm{q} \triangleq \begin{bmatrix} \frac{1}{L_\mathrm{q}} & \frac{L_\mathrm{d}}{L_\mathrm{q}} & \frac{\Phi_\mathrm{pm}}{L_\mathrm{q}} \end{bmatrix}^\top \in \mathbb{R}^3$. Thus the motor current dynamics, i.e. the first two rows of (2), can be rewritten in linearly parameterized form, particularly,

$$\begin{aligned} \dot{i}_\mathrm{d} &= \boldsymbol{\psi}_\mathrm{d}\boldsymbol{\theta}_\mathrm{d} = (-Ri_\mathrm{d} + u_\mathrm{d})\frac{1}{L_\mathrm{d}} + p\omega i_\mathrm{q}\frac{L_\mathrm{q}}{L_\mathrm{d}}, \\ \dot{i}_\mathrm{q} &= \boldsymbol{\psi}_\mathrm{q}\boldsymbol{\theta}_\mathrm{q} = (-Ri_\mathrm{q} + u_\mathrm{q})\frac{1}{L_\mathrm{q}} - p\omega i_\mathrm{d}\frac{L_\mathrm{d}}{L_\mathrm{q}} - p\omega\frac{\Phi_\mathrm{pm}}{L_\mathrm{q}}, \end{aligned} \tag{3}$$

where $\boldsymbol{\psi}_\mathrm{d} \triangleq \begin{bmatrix} -Ri_\mathrm{d} + u_\mathrm{d} & p\omega i_\mathrm{q} \end{bmatrix} \in \mathbb{R}^{1\times 2}$ and $\boldsymbol{\psi}_\mathrm{q} \triangleq \begin{bmatrix} -Ri_\mathrm{q} + u_\mathrm{q} & -p\omega i_\mathrm{d} & -p\omega \end{bmatrix} \in \mathbb{R}^{1\times 3}$.

From the theory of adaptive observers [13], [14], one can formulate an adaptive parameter estimator as follows:

$$\dot{\hat{i}}_\mathrm{d} = \boldsymbol{\psi}_\mathrm{d}\hat{\boldsymbol{\theta}}_\mathrm{d} + \boldsymbol{\mu}_\mathrm{d}^\top\dot{\hat{\boldsymbol{\theta}}}_\mathrm{d} + K_{\mathrm{L_d}}(i_\mathrm{d} - \hat{i}_\mathrm{d}), \tag{4a}$$

$$\dot{\hat{\boldsymbol{\theta}}}_\mathrm{d} = \boldsymbol{\Gamma}_\mathrm{d}\boldsymbol{\mu}_\mathrm{d}(i_\mathrm{d} - \hat{i}_\mathrm{d}),\ \dot{\boldsymbol{\mu}}_\mathrm{d} = -K_{\mathrm{L_d}}\boldsymbol{\mu}_\mathrm{d} + \boldsymbol{\psi}_\mathrm{d}^\top, \tag{4b}$$

$$\dot{\hat{i}}_\mathrm{q} = \boldsymbol{\psi}_\mathrm{q}\hat{\boldsymbol{\theta}}_\mathrm{q} + \boldsymbol{\mu}_\mathrm{q}^\top\dot{\hat{\boldsymbol{\theta}}}_\mathrm{q} + K_{\mathrm{L_q}}(i_\mathrm{q} - \hat{i}_\mathrm{q}), \tag{4c}$$

$$\dot{\hat{\boldsymbol{\theta}}}_\mathrm{q} = \boldsymbol{\Gamma}_\mathrm{q}\boldsymbol{\mu}_\mathrm{q}(i_\mathrm{q} - \hat{i}_\mathrm{q}),\ \dot{\boldsymbol{\mu}}_\mathrm{q} = -K_{\mathrm{L_q}}\boldsymbol{\mu}_\mathrm{q} + \boldsymbol{\psi}_\mathrm{q}^\top, \tag{4d}$$

where $K_{\mathrm{L_d}}, K_{\mathrm{L_q}} > 0$ are some prescribed observer gains, $\boldsymbol{\mu}_\mathrm{d} \in \mathbb{R}^2, \boldsymbol{\mu}_\mathrm{q} \in \mathbb{R}^3$ are the states of the observer, representing the adaptive gain vectors, and $\hat{\boldsymbol{\theta}}_\mathrm{d} \in \mathbb{R}^2$ and $\hat{\boldsymbol{\theta}}_\mathrm{q} \in \mathbb{R}^3$ are the estimation of $\boldsymbol{\theta}$. $\boldsymbol{\Gamma}_\mathrm{d} \in \mathbb{R}^{2\times 2}$ and $\boldsymbol{\Gamma}_\mathrm{q} \in \mathbb{R}^{3\times 3}$ are some

positive definite adaptation gain matrices. One can rewrite (4a) and (4c) as follows:

$$\dot{\hat{i}}_{\mathrm{d}} = \boldsymbol{\psi}_{\mathrm{d}}\hat{\boldsymbol{\theta}}_{\mathrm{d}} + (\boldsymbol{\mu}_{\mathrm{d}}^{\top}\boldsymbol{\Gamma}_{\mathrm{d}}\boldsymbol{\mu}_{\mathrm{d}} + K_{\mathrm{L_d}})(i_{\mathrm{d}} - \hat{i}_{\mathrm{d}}), \tag{5a}$$

$$\dot{\hat{i}}_{\mathrm{q}} = \boldsymbol{\psi}_{\mathrm{q}}\hat{\boldsymbol{\theta}}_{\mathrm{q}} + (\boldsymbol{\mu}_{\mathrm{q}}^{\top}\boldsymbol{\Gamma}_{\mathrm{q}}\boldsymbol{\mu}_{\mathrm{q}} + K_{\mathrm{L_q}})(i_{\mathrm{q}} - \hat{i}_{\mathrm{q}}). \tag{5b}$$

By definition, the estimates of the motor parameters are given by $\hat{\boldsymbol{\beta}} \triangleq \begin{bmatrix} 1/\hat{\boldsymbol{\theta}}_{\mathrm{d}}[1] & 1/\hat{\boldsymbol{\theta}}_{\mathrm{q}}[1] & \hat{\boldsymbol{\theta}}_{\mathrm{q}}[3]/\hat{\boldsymbol{\theta}}_{\mathrm{q}}[1] \end{bmatrix}^{\top}$. The gain selection and tuning strategy is in [14, Section II.C].

Remark 3. *Adaptive parameter estimator design follows [14] where the zero solution of the state and parameter estimation error dynamics is globally exponentially stable as long as the persistent excitation (PE) condition [13, Theorem 5.3.1] holds.*

B. Torque Capacity Modeling Module

Given the common max torque per ampere control (MTPA) strategy [15] for the motor, the motor torque bound can be represented as various analytic functions of speed according to three cases, depending on the sign of $\Phi_{\mathrm{pm}}/L_{\mathrm{d}} - I_{\max}$ [16]. The max torque function with $\Phi_{\mathrm{pm}}/L_{\mathrm{d}} - I_{\max} < 0$ is exemplified as follows:

$$\tau_{\mathrm{m}}(\omega, \boldsymbol{\beta}) = \begin{cases} 1.5p\Phi_{\mathrm{pm}} I_{\max}, & \text{if } |\omega| \le \omega_{\mathrm{r}}, \\ 1.5p\Phi_{\mathrm{pm}} i_{\mathrm{q,lim}}, & \text{if } |\omega| \in [\omega_{\mathrm{r}}, \omega_{\mathrm{s}}], \\ 1.5p\Phi_{\mathrm{pm}} i_{\mathrm{q,lim,V}}, & \text{if } |\omega| \in [\omega_{\mathrm{s}}, \infty), \end{cases} \tag{6}$$

where $\omega_{\mathrm{r}}(\boldsymbol{\beta})$ and $\omega_{\mathrm{s}}(\boldsymbol{\beta})$ are given by

$$\omega_{\mathrm{r}} = \frac{V_{\mathrm{dq,max}}}{p\sqrt{(L_{\mathrm{q}} I_{\max})^2 + \Phi_{\mathrm{pm}}^2}}, \omega_{\mathrm{s}} = \frac{V_{\mathrm{dq,max}}}{p\sqrt{(L_{\mathrm{d}} I_{\max})^2 - \Phi_{\mathrm{pm}}^2}};$$

$i_{\mathrm{q,lim,V}}(\omega, \boldsymbol{\beta})$ and $i_{\mathrm{q,lim}}(\omega, \boldsymbol{\beta})$ are given by

$$i_{\mathrm{q,lim,V}} = V_{\mathrm{dq,max}}/(p\omega L_{\mathrm{q}}), \; i_{\mathrm{q,lim}} = \sqrt{I_{\max}^2 - i_{\mathrm{d,lim}}^2},$$

$$i_{\mathrm{d,lim}} = \frac{(V_{\mathrm{dq,max}}/(p\omega))^2 - (L_{\mathrm{d}} I_{\max})^2 - \Phi_{\mathrm{pm}}^2}{2\Phi_{\mathrm{pm}} L_{\mathrm{d}}}.$$

This piecewise-defined function is visualized in Fig. 3. The black dashed horizontal line represents the constant max torque $\tau_{\mathrm{m},c}(\boldsymbol{\beta}) \triangleq 1.5p\Phi_{\mathrm{pm}} I_{\max}$ given by the first row of (6). The yellow and grey dash-dot vertical lines represent $\omega_{\mathrm{r}}(\boldsymbol{\beta})$ and $\omega_{\mathrm{s}}(\boldsymbol{\beta})$, respectively. The blue and brown dashed curves represent the max torque based on the second and third rows of (6), respectively. Regardless of the sign of $\Phi_{\mathrm{pm}}/L_{\mathrm{d}} - I_{\max}$, the following properties always hold:

1) $\tau_{\mathrm{m}}(\omega, \boldsymbol{\beta})$ is a constant, i.e. the constant max torque $\tau_{\mathrm{m},c}(\boldsymbol{\beta}) \triangleq 1.5p\Phi_{\mathrm{pm}} I_{\max}$, when $\omega \in [0, \omega_{\mathrm{r}}(\boldsymbol{\beta})]$;
2) $\omega_{\mathrm{m}}(\boldsymbol{\beta}) > \omega_{\mathrm{r}}(\boldsymbol{\beta})$ is the max motor speed and $\omega_{\mathrm{m}}(\boldsymbol{\beta}) = \infty$ when $\Phi_{\mathrm{pm}}/L_{\mathrm{d}} - I_{\max} \le 0$.
3) $\tau_{\mathrm{m}}(\omega, \boldsymbol{\beta})$ is monotonically decreasing when $\omega \in [\omega_{\mathrm{r}}(\boldsymbol{\beta}), \omega_{\mathrm{m}}(\boldsymbol{\beta})]$; $\tau_{\mathrm{m}} = 0$ when $\omega = \omega_{\mathrm{m}}$;
4) when $\omega < 0$, $\tau_{\mathrm{m}}(\omega, \boldsymbol{\beta}) = \tau_{\mathrm{m}}(-\omega, \boldsymbol{\beta})$.

Given motor speed ω, desired torque τ_{des} and torque analytical bound such as (6), the desired motor currents $i_{\mathrm{d,des}}, i_{\mathrm{q,des}}$ can be computed analytically. [16, Algorithm 1] provides the detailed steps of this analytical method, which is referred to as "Torque-Speed To Current" in Fig. 1 and Fig. 2.

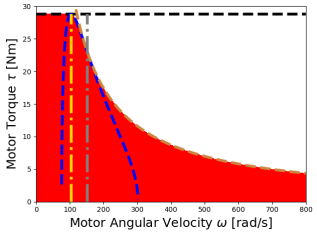

Fig. 3. Motor torque bound for case $\Phi_{\mathrm{pm}}/L_{\mathrm{d}} < I_{\max}$. The red and white region represents the feasible and infeasible operation range, respectively.

C. Reference Reshaper

Given the motor parameter estimates from the adaptive estimator, the torque capacity modeling module provides the necessary information, which is further fed into the proposed reference reshaper (RR) to adjust the possibly infeasible reference as a dynamically feasible trajectory for accurate tracking. Unlike the classic reference/command governor that solves a constrained optimization for every reference point with a maximal constraint admissible set defined explicitly [5], the RR first formulates a similar optimization but then searches over a finite set of critical points (at most six) for the optimal solution. A computationally efficient algorithm is proposed for the implementation of RR and a theoretical analysis of the algorithm is provided.

At each timestamp t_k, given the desired acceleration (from the motion planner) $a_{\mathrm{des},k+1} \triangleq a_{\mathrm{des}}(t_{k+1})$ for duration $[t_k, t_{k+1})$, $(t_{k+1} = t_k + \Delta)$, the reference reshaper is the following constrained optimization, which finds the closest desired acceleration subject to the torque constraint,

$$a^*_{\mathrm{des},k+1} = \underset{a_{k+1}}{\arg\min} \quad ||a_{k+1} - a_{\mathrm{des},k+1}||^2 \tag{7a}$$

$$\text{s.t.} \quad |a_{k+1}/Z| \le \tau_{\mathrm{m}}(\omega_{k+1}), \tag{7b}$$

$$\omega_{k+1} = \tfrac{v_k + \Delta a_{k+1}}{ZJ}. \tag{7c}$$

Note that the RR runs for every time interval Δ. The above problem can be rewritten by changing the decision variable as ω_{k+1} and imposing an additional constraint $|\omega_{k+1}| \le \omega_{\mathrm{m}}(\boldsymbol{\beta})$ to account for the ω constraint (1b), i.e.

$$\min_{\omega_{k+1}} \quad F(\omega_{k+1}) := ||(\frac{ZJ}{\Delta}\omega_{k+1} - \frac{v_k}{\Delta}) - a_{\mathrm{des},k+1}||^2 \tag{8a}$$

$$\text{s.t.} \quad |\frac{J}{\Delta}\omega_{k+1} - \frac{v_k}{Z\Delta}| \le \gamma\tau_{\mathrm{m}}(\omega_{k+1}), \tag{8b}$$

$$-\omega_{\mathrm{m}}(\boldsymbol{\beta}) \le \omega_{k+1} \le \omega_{\mathrm{m}}(\boldsymbol{\beta}), \tag{8c}$$

where $\gamma \in (0, 1]$ is a prescribed torque margin constant near 1, permitting a slight overshoot in the tracking controller that will be introduced in Sec. III-D. If the optimal motor speed from (8) is given by ω^*_{k+1}, then the optimal desired motions are $a^*_{\mathrm{des},k+1} = (ZJ\omega^*_{k+1} - v_k)/\Delta$, $v^*_{\mathrm{des},k+1} = ZJ\omega^*_{k+1}$, and $s^*_{\mathrm{des},k+1} = s_k + v_k\Delta + 0.5a^*_{\mathrm{des},k+1}\Delta^2$.

Solving either (7) or (8) for every reference point $a_{\mathrm{des},k+1}$ may be computationally expensive. Thus, by checking the KKT (Karush–Kuhn–Tucker) necessary conditions on the

optimization problem (8), one can search over only a finite set of critical points (at most six) of motor speed for the optimal solution of (8). To begin with, the optimal w^*_{k+1} must either be a stationary point of the objective function (8a), or lie on the boundary of the feasible region. If w^*_{k+1} is a stationary point of the objective function, it must be $\omega^*_{k+1} = (v_k + \Delta a_{\mathrm{des},k+1})/(ZJ)$. On the other hand, if w^*_{k+1} lies on the boundary of the feasible region, then $w^*_{k+1} \in \Omega_{\mathrm{L}} \cup \Omega_{\mathrm{U}} \cup \{\pm\omega_{\mathrm{m}}(\beta)\}$, where $\Omega_{\mathrm{L}} \triangleq \{\omega | \xi_{\mathrm{L}}(\omega) := \gamma\tau_{\mathrm{m}}(\omega) + (\frac{J}{\Delta}\omega - \frac{v_k}{Z\Delta}) = 0\}$ and $\Omega_{\mathrm{U}} \triangleq \{\omega | \xi_{\mathrm{U}}(\omega) := \gamma\tau_{\mathrm{m}}(\omega) - (\frac{J}{\Delta}\omega - \frac{v_k}{Z\Delta}) = 0\}$ are the roots of constraints (8b) when they are active.

From a geometric perspective, Fig. 4 illustrates the optimization (8). The slope and the intercept of the red line are fixed given a particular v_k. The possible a_{k+1} can be any points along the red line segment intersected with the torque bound $\tau_{\mathrm{m}}(\omega_{k+1})$ and $-\tau_{\mathrm{m}}(\omega_{k+1})$. The optimal a^*_{k+1} is the point with the minimal distance to the desired acceleration $a_{\mathrm{des},k+1}$ (in green dotted line). Since the slope ZJ/Δ of the red line cannot be zero, Ω_{L} and Ω_{U} must contain only one point, respectively. Algorithm 1 summarizes the implementation details. As discussed above, Line 2 constructs the set $\{\frac{v_k+\Delta a_{\mathrm{des},k+1}}{ZJ}\} \cup \Omega_{\mathrm{U}} \cup \Omega_{\mathrm{L}} \cup \{\pm\omega_{\mathrm{m}}(\hat{\boldsymbol{\beta}}), \omega_k\}$ as the solution candidates to (8), where ω_k is included to contain an element that always satisfies all the primal constraints. Line 3 filters out the infeasible solutions in Ω to obtain the set of feasible candidates $\bar{\Omega}$. Finally, Line 4-5 return the element in $\bar{\Omega}$ with the lowest objective value as the optimal motor speed ω^*_{k+1}, and the optimal desired motions.

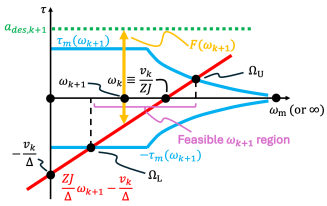

Fig. 4. A geometric illustration of the optimization (8).

Algorithm 1: Reference Reshaper

Input: $\omega_k, v_k, s_k, a_{\mathrm{des},k+1}, \hat{\boldsymbol{\beta}}, \Delta, \gamma, Z, J$

1 Solve the root Ω_{L} and Ω_{U}

2 $\Omega \leftarrow \{\frac{v_k+\Delta a_{\mathrm{des},k+1}}{ZJ}\} \cup \Omega_{\mathrm{U}} \cup \Omega_{\mathrm{L}} \cup \{\pm\omega_{\mathrm{m}}(\hat{\boldsymbol{\beta}}), \omega_k\}$

3 $\bar{\Omega} \leftarrow \{\omega \in \Omega : |\omega| \le \omega_{\mathrm{m}}(\hat{\boldsymbol{\beta}}),\ |\frac{J}{\Delta}\omega - \frac{v_k}{Z\Delta}| \le \gamma\tau_{\mathrm{m}}(\omega)\}$

4 $\omega^*_{k+1} \leftarrow \arg\min_{\omega\in\bar{\Omega}} F(\omega)$, $a^*_{\mathrm{des},k+1} \leftarrow (ZJ\omega^*_{k+1} - v_k)/\Delta$

5 $v^*_{\mathrm{des},k+1} \leftarrow ZJ\omega^*_{k+1}$, $s^*_{\mathrm{des},k+1} \leftarrow s_k + \frac{(v^*_{\mathrm{des},k+1}+v_k)\Delta}{2}$

The following theorem guarantees the algorithm's optimality, and the proof is provided in the Appendix.

Theorem 1. *By searching over the finite set of solution candidates $\bar{\Omega}$, the solution returned by Algorithm 1 is the optimal solution of optimization problems (7) and (8).*

D. Position & Current Tracking Controller

Given $a_{\mathrm{des}}(t)$, $v_{\mathrm{des}}(t)$, and $s_{\mathrm{des}}(t)$ from the motion planner or the reshaped ones with superscript * from the reference reshaper, the position tracking controller calculates the desired motor torque by $\tau_{\mathrm{des}}(t) = \frac{a_{\mathrm{des}}(t)}{Z} - K_{\mathrm{P},\tau}e_s(t) - K_{\mathrm{I},\tau}\int_0^t e_s(t)dt - K_{\mathrm{D},\tau}e_v(t)$, where $e_s(t) \triangleq s(t) - s_{\mathrm{des}}(t)$, $e_v(t) \triangleq v(t) - v_{\mathrm{des}}(t)$. Given $i_{\mathrm{d,des}}(t)$ and $i_{\mathrm{q,des}}(t)$ returned by the "Torque-Speed To Current" module, along with $\tau_{\mathrm{des}}(t)$ and $\omega(t)$, the motor voltage is calculated to track $i_{\mathrm{d,des}}(t)$ and $i_{\mathrm{q,des}}(t)$: $u_{\mathrm{d,des}}(t) = Ri_{\mathrm{d,des}}(t) - \hat{L}_{\mathrm{q}}p\omega(t)i_{\mathrm{q}}(t) - K_{\mathrm{P},i_{\mathrm{d}}}e_{i_{\mathrm{d}}}(t) - K_{\mathrm{I},i_{\mathrm{d}}}\int_0^t e_{i_{\mathrm{d}}}(t)dt$, $u_{\mathrm{q,des}}(t) = Ri_{\mathrm{q,des}}(t) + (\hat{L}_{\mathrm{d}}i_{\mathrm{d}}(t) + \hat{\Phi}_{\mathrm{pm}})p\omega(t) - K_{\mathrm{P},i_{\mathrm{q}}}e_{i_{\mathrm{q}}}(t) - K_{\mathrm{I},i_{\mathrm{q}}}\int_0^t e_{i_{\mathrm{q}}}(t)dt$, where $e_{i_{\mathrm{d}}}(t) \triangleq i_{\mathrm{d}}(t) - i_{\mathrm{d,des}}(t)$, $e_{i_{\mathrm{q}}}(t) \triangleq i_{\mathrm{q}}(t) - i_{\mathrm{q,des}}(t)$.

IV. Simulation

This section presents simulation results to validate the proposed framework. The parameters are: $p = 4$, $R = 0.08\ \Omega$, $J = 0.15\ \mathrm{kg}\cdot\mathrm{m}^2$, $Z = 0.05$, $I_{\max} = 40$ A, $V_{\max} = 100\sqrt{3}$ V, $\Delta = 1$ ms, $\gamma = 0.97$. The gains are: $K_{\mathrm{L_d}} = 300$, $K_{\mathrm{L_q}} = 200$, $\boldsymbol{\Gamma}_{\mathrm{d}} = \mathrm{diag}\{3570, 600\}$, $\boldsymbol{\Gamma}_{\mathrm{q}} = \mathrm{diag}\{33000, 900, 660\}$. The system dynamics (2) and parameter estimator dynamics (4) are forward propagated given Euler integration with time step $\Delta_{\mathrm{s}} = 0.1$ ms. The motor's true torque bound is shown in Fig. 3.

A. Adaptive Parameter Estimator

Let $L_{\mathrm{d}} = L_{\mathrm{q}} = 5$ mH, and $\Phi_{\mathrm{pm}} = 120$ mWb. Let the initial parameter estimate (pre-calibrated value) include a 10% error. First, a prescribed trajectory for $i_{\mathrm{d,des}}(t)$ and $i_{\mathrm{q,des}}(t)$ is given to the proposed closed-loop system, serving as a cold start for the adaptive parameter estimator. The magnitude of $i_{\mathrm{d,des}}(t)$ and $i_{\mathrm{q,des}}(t)$ is designed to remain sufficiently small to ensure that no constraints are violated. To satisfy the PE condition, the trajectory of $i_{\mathrm{d,des}}$ and $i_{\mathrm{q,des}}$ contains sinusoidal signals with 7 distinct frequencies respectively. The proposed framework tracks $i_{\mathrm{d,des}}$ and $i_{\mathrm{q,des}}$ based on the real-time parameter estimate $\hat{\boldsymbol{\beta}}$, which is continually updated using the adaptive parameter estimator (4) with a sampling interval of $\Delta_{\mathrm{s}} = 0.1$ ms. The trajectory of parameter estimates and true values is shown in Fig. 5. The final estimation error for $L_{\mathrm{d}}, L_{\mathrm{q}}, \Phi_{\mathrm{pm}}$ is 1.68×10^{-4} mH (0.00%), 4.44×10^{-3} mH (0.01%), and 1.22×10^{-2} mWb (0.01%), respectively.

B. Reference Reshaper

The stroke of the desired motion is 3 m. The motion planner in both Fig. 1 and Fig. 2 generates time-optimal desired motion trajectories in a bang-bang control fashion: a max acceleration a_{m} is applied until it reaches the half stroke or a max velocity v_{m}; travel with constant max velocity if the half stroke is not reached yet; then reverse this process for deceleration to reach the terminal position with zero terminal

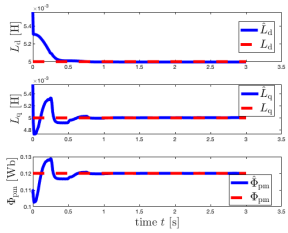

Fig. 5. The trajectory of motor parameters' true values and estimates.

velocity. The default value of a_{m} is set to $\tau_{\mathrm{m},c}(\boldsymbol{\beta})/Z = 1.44$ m/s^2, with $\tau_{\mathrm{m},c}(\boldsymbol{\beta}) = 28.8$ N $\cdot$ m, as illustrated in Fig. 3. $v_{\mathrm{m}} = 5$ m/s. The methods used are summarized as follows:

1) B1, baseline (faster) in Fig. 1, true motor parameters;
2) B2, baseline (slower) in Fig. 1, true motor parameters;
3) P1, proposed in Fig. 2, true motor parameters;
4) P2, proposed in Fig. 2, estimated motor parameters.

As illustrated in Fig. 3, the constant max torque cannot be applied continually because the max torque decreases when $\omega > \omega_{\mathrm{r}}$. The default motion planner contains dynamically infeasible acceleration due to this attribute. Fig. 6a demonstrates that when the motion planner provides an aggressive initial reference trajectory (dashed red line), B1, without the RR in place, can only generate a torque trajectory following the solid blue line, indicating that the reference trajectory is infeasible. An infeasible τ_{des} results in infeasible $i_{\mathrm{d,des}}, i_{\mathrm{q,des}}$, which prevents the motor current controller from tracking them within bounded $u_{\mathrm{d}}, u_{\mathrm{q}}$. The spike of the actual torque trajectory in blue at 2.3 s indicates the violation of motor current and voltage constraints. By empirically reducing 30% of $a_{\mathrm{m}} = 1.44$ m/s^2, a less aggressive initial reference trajectory (in dashed magenta of Fig. 6a) produces a torque trajectory in solid cyan without violating any constraints, but still suffers from infeasibility. As Table II shows, the aggressive and dynamically infeasible reference trajectory of B1 produces a large final position error; the less aggressive trajectory of B2 leads to a relatively large final position error and a relatively longer motion.

TABLE II
PERFORMANCE SUMMARY FOR REFERENCE RESHAPER

Index	B1	B2	P1	P2
Violated V & I constraints	Y	***N***	***N***	***N***
Max Acceleration [m/s^2]	**1.44**	1.00	**1.44**	**1.44**
Motion Time [s]	~~2.9277~~†	3.4641	**3.0607**	**3.0607**
Final Pos. Error [mm]	205.1	16.1	**0.9**	2.6
Avg. RR Comp. Time [ms]	N/A	N/A	1.18	1.26

†: strikethrough indicates constraint violation

Fig. 6b presents the case with RR (P2), where the desired torque trajectory is obtained by reshaping the very aggressive initial trajectory (of B1) in Fig. 6a. The true trajectory tracks the reshaped desired trajectory closely, which implies the recovery of dynamical feasibility by the RR. By Table II, P1 and P2 yield the smallest motion time. With the estimated motor parameters, P2 has a similar final position error, compared to P1 with true parameters. Without any code optimization, a basic MATLAB implementation of Algorithm 1 results in an average computation time of approximately 1 ms for the RR. Even though this is slightly longer than $\Delta = 1$ ms, it is anticipated that implementing Algorithm 1 in C++ with code optimization will reduce the computation time to within 1 ms. A naive implementation of RR by solving the optimization (7a) via IPOPT yields an average computation time of 9.92 ms. Fig. 6c provides the desired motion trajectory before (dashed red) and after (dashed magenta) reshaping and the actual motion (solid blue) tracking of the reshaped desired trajectory. The discrepancy between the dashed red and the dashed magenta indicates the dynamical infeasibility of the original aggressive reference trajectory. On the other hand, the actual motion in solid blue indicates the effectiveness of the proposed reference reshaper given estimated motor parameters.

V. CONCLUSION AND FUTURE WORK

Aiming to address the conservativeness or dynamical infeasibility of conventional trajectory generation methods for servo systems, this paper proposes a method that first performs stable adaptive estimation of the servomotor model parameters, then establishes the torque capacity constraints as analytical functions of the speed based on parameter estimates, and finally develops a computationally efficient algorithm to reshape an aggressive (dynamically infeasible) trajectory into a feasible one according to the constraints. Future work includes the improvement of the algorithm's computational efficiency, the experimental validation, and the extension to multi-axis servo systems.

APPENDIX

Proof of Theorem 1. The Lagrangian of (8) is written by

$$\begin{aligned} L(w_{k+1}, \boldsymbol{\lambda}) &= ||(\frac{ZJ}{\Delta}\omega_{k+1} - \frac{v_k}{\Delta}) - a_{\mathrm{des},k+1}||^2 \\ &+ \lambda_1((\frac{J}{\Delta}\omega_{k+1} - \frac{v_k}{Z\Delta}) - \gamma\tau_{\mathrm{m}}(\omega_{k+1})) \\ &+ \lambda_2(-(\frac{J}{\Delta}\omega_{k+1} - \frac{v_k}{Z\Delta}) - \gamma\tau_{\mathrm{m}}(\omega_{k+1})) \\ &+ \lambda_3(\omega_{k+1} - \omega_{\mathrm{m}}(\beta)) + \lambda_4(-\omega_{k+1} - \omega_{\mathrm{m}}(\beta)), \end{aligned} \tag{9}$$

where $\boldsymbol{\lambda} = \begin{bmatrix}\lambda_1 & \lambda_2 & \lambda_3 & \lambda_4\end{bmatrix}^\top \in \mathbb{R}^4$ is the Lagrange multiplier. Denote $\dot{\tau}_{k+1} \triangleq \frac{\partial\tau_{\mathrm{m}}(\omega)}{\partial\omega}|_{\omega=\omega_{k+1}}$. The KKT necessary conditions of (8) are

$$\begin{aligned} &\frac{2ZJ}{\Delta}((\frac{ZJ}{\Delta}\omega_{k+1} - \frac{v_k}{\Delta}) - a_{\mathrm{des},k+1}) + \lambda_1(-\gamma \\ &\dot{\tau}_{k+1} + \frac{J}{\Delta}) + \lambda_2(-\gamma\dot{\tau}_{k+1} - \frac{J}{\Delta}) + \lambda_3 - \lambda_4 = 0, \end{aligned} \tag{10a}$$

$$\lambda_1((\frac{J}{\Delta}\omega_{k+1} - \frac{v_k}{Z\Delta}) - \gamma\tau_{\mathrm{m}}(\omega_{k+1})) = 0, \tag{10b}$$

$$\lambda_2(-(\frac{J}{\Delta}\omega_{k+1} - \frac{v_k}{Z\Delta}) - \gamma\tau_{\mathrm{m}}(\omega_{k+1})) = 0, \tag{10c}$$

$$\lambda_3(\omega_{k+1} - \omega_{\mathrm{m}}(\beta)) = 0,\ \lambda_4(-\omega_{k+1} - \omega_{\mathrm{m}}(\beta)) = 0, \tag{10d}$$

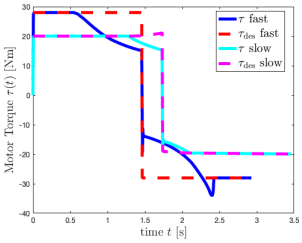

(a) Desired and actual torque trajectory given high (B1) and low (B2) acceleration.

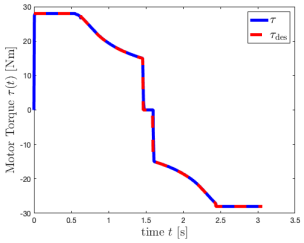

(b) Desired and actual torque trajectory given high acceleration with reference reshaper (P2).

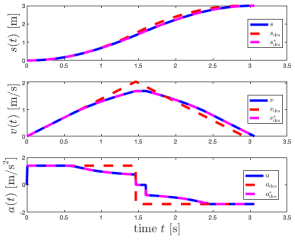

(c) Desired motion before (with $_{\text{des}}$) and after reference reshaper (with *) vs actual motion (P2).

Fig. 6. Desired and actual torque and motion trajectory of different methods.

$$\lambda_1, \lambda_2, \lambda_3, \lambda_4 \geq 0, \tag{10e}$$

$$(\frac{J}{\Delta}\omega_{k+1} - \frac{v_k}{Z\Delta}) - \gamma\tau_{\text{m}}(\omega_{k+1}) \leq 0, \tag{10f}$$

$$-(\frac{J}{\Delta}\omega_{k+1} - \frac{v_k}{Z\Delta}) - \gamma\tau_{\text{m}}(\omega_{k+1}) \leq 0, \tag{10g}$$

$$\omega_{k+1} - \omega_{\text{m}}(\beta) \leq 0, \ -\omega_{k+1} - \omega_{\text{m}}(\beta) \leq 0. \tag{10h}$$

The optimal solution to (8) must lie in the solutions to (10). The following analyzes the solutions to (10) and then determines the solution to (8). The possible solutions of (10) are divided into three cases depending on the values of $\boldsymbol{\lambda}$.

Case A: $\lambda_1 = \lambda_2 = \lambda_3 = \lambda_4 = 0$. This case corresponds to the scenario where all the primal constraints are inactive. In this case, (10a) reduces to

$$\omega^*_{k+1} = (v_k + \Delta a_{\text{des},k+1})/(ZJ). \tag{11}$$

Note the objective function value of (8) given the ω^*_{k+1} in (11) is exactly 0. Therefore, if (11) satisfies all the primal constraints, then it is the optimal solution to (8).

Case B: $\lambda_i > 0$ for some $i \in \{1, 2, 3, 4\}$. This case corresponds to the scenario where some primal constraints are active. In this case, w^*_{k+1} lies on the boundary of the feasible region. Recall Ω_{L} and Ω_{U} are the roots of (10f) and (10g) when the equality is achieved. Then in Case B, the candidate w^*_{k+1} falls into the set of $\Omega_{\text{L}} \cup \Omega_{\text{U}} \cup \{\pm\omega_{\text{m}}(\beta)\}$. As illustrated in Fig. 4, ZJ/Δ and J/Δ cannot be zero. Thus, $\Omega_{\text{L}} \triangleq \{\omega | \xi_{\text{L}}(\omega) := \gamma\tau_{\text{m}}(\omega) + (\frac{J}{\Delta}\omega - \frac{v_k}{Z\Delta}) = 0\}$ and $\Omega_{\text{U}} \triangleq \{\omega | \xi_{\text{U}}(\omega) := \gamma\tau_{\text{m}}(\omega) - (\frac{J}{\Delta}\omega - \frac{v_k}{Z\Delta}) = 0\}$ only contains at most one point, respectively.

Case C: This case corresponds to the scenario with no feasible solution to (8), i.e. the constraints (8b) and (8c) might be violated. In other words, there exists no acceleration to further increase the motor speed from ω_k to ω_{k+1}. Thus, the solution in this case is ω_k.

By combining all three cases, as Line 1-2 of Algorithm 1 state, one can construct the solution candidate set Ω, which contains all the possible solutions of the necessary conditions (10). The optimal solution to (8) must lie in the solution candidate set Ω. Then, by filtering the feasible solution candidate set as $\bar{\Omega}$ and sorting the objective function value $F(\omega)$ of each candidate in $\bar{\Omega}$, one can obtain the optimal solution to (8), which is equivalent to the problem (7) by changing the decision variable. This completes the proof. ■

REFERENCES

[1] K. D. Nguyen, T.-C. Ng, and I.-M. Chen, "On algorithms for planning s-curve motion profiles," *Int. J. Adv. Ro. Sys.*, vol. 5, no. 1, p. 11, 2008.

[2] Y. Wang, K. Ueda, and S. A. Bortoff, "A hamiltonian approach to compute an energy efficient trajectory for a servomotor system," *Automatica*, vol. 49, no. 12, pp. 3550–3561, 2013.

[3] Y. Wang, Y. Zhao, S. A. Bortoff, and K. Ueda, "A real-time energy-optimal trajectory generation method for a servomotor system," *IEEE Trans. Ind. Electron.*, vol. 62, no. 2, pp. 1175–1188, 2014.

[4] D. Lam, C. Manzie, and M. C. Good, "Model predictive contouring control for biaxial systems," *IEEE Trans. Ctrl. Sys. Tech.*, vol. 21, no. 2, pp. 552–559, 2012.

[5] S. Di Cairano, A. Goldsmith, U. V. Kalabić, and S. A. Bortoff, "Cascaded reference governor–mpc for motion control of two-stage manufacturing machines," *IEEE Trans. Ctrl. Sys. Tech.*, vol. 27, no. 5, pp. 2030–2044, 2018.

[6] S. Balula, D. Liao-McPherson, A. Rupenyan, and J. Lygeros, "Data-driven reference trajectory optimization for precision motion systems," *Control Engineering Practice*, vol. 144, p. 105834, 2024.

[7] Y. Liu, Z. Chen, and B. Yao, "Constrained time-optimal adaptive robust control of linear motors using an indirect method," in *IEEE 18th Intl. Conf. on Autom. Sci. & Eng. (CASE)*, 2022, pp. 2335–2340.

[8] H. K. Khalil, E. G. Strangas, and S. Jurkovic, "Speed observer and reduced nonlinear model for sensorless control of induction motors," *IEEE Trans. Ctrl. Sys. Tech.*, vol. 17, no. 2, pp. 327–339, 2008.

[9] D. M. Reed, J. Sun, and H. F. Hofmann, "Simultaneous identification and adaptive torque control of permanent magnet synchronous machines," *IEEE Trans. Ctrl. Sys. Tech.*, vol. 25, no. 4, pp. 1372–1383, 2016.

[10] C. Chatri, M. Labbadi, M. Ouassaid, K. Elyaalaoui, and Y. El Houm, "Design and implementation of finite-time control for speed tracking of permanent magnet synchronous motors," *IEEE Control Systems Letters*, vol. 7, pp. 721–726, 2022.

[11] Y. W. Jeong and C. C. Chung, "Nonlinear proportional-integral disturbance observers for motion control of permanent magnet synchronous motors," *IEEE Control Systems Letters*, vol. 6, pp. 3062–3067, 2022.

[12] E. Garone, S. Di Cairano, and I. Kolmanovsky, "Reference and command governors for systems with constraints: A survey on theory and applications," *Automatica*, vol. 75, pp. 306–328, 2017.

[13] P. A. Ioannou and J. Sun, *Robust adaptive control*. PTR Prentice-Hall Upper Saddle River, NJ, 1996.

[14] Q. Zhang, "Adaptive observer for multiple-input-multiple-output (MIMO) linear time-varying systems," *IEEE Trans. Autom. Control*, vol. 47, no. 3, pp. 525–529, Mar. 2002.

[15] A. Consoli, G. Scarcella, G. Scelba, and A. Testa, "Steady-state and transient operation of ipmsms under maximum-torque-per-ampere control," *IEEE Trans. on Ind. Appl.*, vol. 46, no. 1, pp. 121–129, 2009.

[16] Z. Lu and Y. Wang, "A differentiable dynamic modeling approach to integrated motion planning and actuator physical design for mobile manipulators," *Journal of Field Robotics*, 2024.